UDC 539.4

Nonlinear Dynamic Finite Element Analysis of Thick Transversely Flexible Sandwich Panel on Elastic Foundation with Account of Damage Progression in Time. Part 2. 3D Analysis and Time Integration*

V. Y. Perel

Air Force Institute of Technology, Department of Aeronautics and Astronautics, Wright Patterson Air Force Base, Ohio, USA

УДК 539.4

Нелинейный динамический конечноэлементный анализ гибкой в поперечном направлении толстой многослойной панели на упругом основании с учетом развития повреждений во времени. Сообщение 2. Трехмерный расчет и интегрирование по времени

В. Ю. Перель

Технологический институт ВВС США, Отделение аэронавтики и астронавтики, Хобсон Бэй, Огайо, США

Для случая толстой многослойной панели с поверхностными слоями из композитного ламината предложена расчетная схема в рамках теории пластин с использованием упрощенных представлений, описанных в сообщении 1. Алгоритм расчета динамической задачи, учитывающий развитие повреждений в материале, используется в расчетной схеме, основанной на геометрически нелинейной формулировке задачи, для анализа условий разрушения многослойной панели, которая подвергается ударному нагружению при падении на грунт.

Ключевые слова: сжимаемые в поперечном направлении многослойные панели, упругое основание, нелинейная динамика, развитие повреждений во времени, трехмерное напряженное состояние.

Introduction. In the present paper, a computational scheme for analysis of the sandwich plate is constructed in which the simplifying assumptions that lead to a plate-type theory are made with respect to the variation of the transverse strains in the thickness direction of the face sheets and the core of the sandwich plate. The displacements are then obtained by integration of these assumed transverse strains, and the constants of integration are chosen to satisfy the conditions of continuity of the displacements across the borders between the face sheets and the core. In such a method, the required continuity of displacements in the thickness direction is satisfied regardless of the assumed type of through-the-thickness distribution of the transverse strains, and the transverse flexibility of the plate can be taken into account. This leads to a larger number of choices of simplifying assumptions about the variation of strains (and, therefore,

* Formulas in Parts 1 and 2 have through numeration.

displacements) in the thickness direction, and, therefore, allows a better adjustment of the computational scheme to the conditions under which the sandwich plate is analyzed by a layerwise method with only three sublaminates (being the face sheets and the core). The transverse stresses are computed by integration of the pointwise equilibrium equations that leads to satisfaction of conditions of continuity of the transverse stresses across the boundaries between the face sheets and the core and satisfaction of stress boundary conditions on the upper and lower surfaces of the plate.

The model is considered on the basis of the simplest of such assumptions that do not ignore, in the expression for the strain energy, the transverse shear and normal strains in the face sheets. It is assumed here that the transverse strains do not vary in the thickness direction within the face sheets and the core, but can be different functions of the in-plane coordinate in the face sheets and the core. In the post-process stage of analysis, these first approximations of the transverse strains can be improved by substituting the transverse stresses, obtained by integration of the pointwise equations of motion (Appendix [1]) into the strain-stress relations. These improved values of the transverse strains vary in the thickness direction and are sufficiently accurate as compared to those of the known exact solutions, based on the linear three-dimensional theory [2–3]. In the theory, discussed in this paper, the transverse displacement, obtained by integration of the assumed transverse normal strain, varies linearly in the thickness direction within a sublaminate (therefore, transverse compressibility of the plate is taken into account), and the in-plane displacement, obtained by integration of the assumed transverse shear strains, varies quadratically within the thickness of a sublaminate. The developed theory does not require many degrees of freedom in finite element models, despite its ability to capture the transverse flexibility of the plate and non-linear through-the-thickness variation of the in-plane displacements.

Three-Dimensional Formulation. The sandwich plate is divided into three conventional layers (sublaminates): the two face sheets and the core. Within each sublaminate, the simplifying assumptions of the plate theory are made separately. In the following text, the superscript k denotes the number of a sublaminate: $k = 1$ denotes the lower face sheet, $k = 2$ denotes the core, and $k = 3$ denotes the upper face sheet (see Fig. 1 in Part 1 [1]).

Finite Element Formulation for Cylindrical Bending. Let us call the dimension of the plate in the x-direction the length, and dimension in the y-direction – the width. If the width of the plate is much larger than its length, and if the load intensity does not vary in the width direction, then the displacements do not depend on the y-coordinate:

$$u = u(x,z), \qquad v = v(x,z), \qquad w = w(x,z). \tag{42}$$

Such a condition is called a generalized plane strain or cylindrical bending. In case of cylindrical bending, the unknown functions depend only on the x-coordinate and time. Therefore, the two-dimensional plate-bending problem reduces to the one-dimensional problem. Then, all derivatives with respect to the y-coordinate vanish in all formulas of the preceding sections.

Hereafter, a sandwich plate will be considered with an isotropic or transversely isotropic core and with face sheets being composite laminates of 0 and 90° plies orientation. In this case, at each point of the plate there is a plane of elastic symmetry

$$u = u(x,z), \qquad w = w(x,z), \qquad v = 0, \tag{43}$$

parallel to the $x - z$ coordinate plane, and, therefore, the condition of the generalized plane strain reduces to the condition of pure plane strain [1], that is, and all strain components, associated with the y-direction, are equal to zero:

$$\varepsilon_{yy} = 0, \qquad \varepsilon_{xy} = 0, \qquad \varepsilon_{yz} = 0. \tag{44}$$

Therefore, the unknown functions are

$$u_0,\ \omega_0,\ \varepsilon_{xz}^{(1)},\ \varepsilon_{zz}^{(1)},\ \varepsilon_{xz}^{(2)},\ \varepsilon_{zz}^{(2)},\ \varepsilon_{xz}^{(3)},\ \varepsilon_{zz}^{(3)}. \tag{45}$$

To perform a finite element formulation, the unknown functions and $w_0(x,t)$ are represented by piecewise interpolation polynomials:

$$u_0 = [M_1 \quad M_2] \begin{Bmatrix} u(0) \\ u(l) \end{Bmatrix}, \tag{46}$$

$$\varepsilon_{xz}^{(k)} = [M_1 \quad M_2] \begin{Bmatrix} \varepsilon_{xz}^{(k)}(0) \\ \varepsilon_{xz}^{(k)}(l) \end{Bmatrix}, \tag{47}$$

where

$$M_1 = 1 - \frac{x}{l}, \qquad M_2 = \frac{x}{l}; \tag{48}$$

$$w_0 = [N_1 \quad N_2 \quad N_3 \quad N_4] \begin{Bmatrix} \omega_0(0) \\ \dfrac{d\omega_0}{dx}(0) \\ \omega_0(l) \\ \dfrac{d\omega_0}{dx}(l) \end{Bmatrix}, \tag{49}$$

and l is a length of a finite element;

$$\varepsilon_{zz}^{(k)} = [N_1 \quad N_2 \quad N_3 \quad N_4] \begin{Bmatrix} \varepsilon_{zz}^{(k)}(0) \\ \dfrac{d\varepsilon_{zz}^{(k)}}{dx}(0) \\ \varepsilon_{zz}^{(k)}(l) \\ \dfrac{d\varepsilon_{zz}^{(k)}}{dx}(l) \end{Bmatrix}, \tag{50}$$

where

$$N_1 = 1 - \frac{3x^2}{l^2} + \frac{2x^3}{l^3}, \quad N_2 = x - \frac{2x^2}{l} + \frac{x^3}{l^2},$$
$$N_3 = \frac{3x^2}{l^2} - \frac{2x^3}{l^3}, \qquad N_4 = -\frac{x^2}{l} + \frac{x^3}{l^2}. \tag{51}$$

Here and further in this section, devoted to the finite element formulation, it is implied for simplicity of notations that x is a coordinate in the element (local) coordinate system, the origin of which coincides with a left node of a finite element. This choice of interpolation polynomials is explained in [2].

Thus, the combined finite element has 24 degrees of freedom. At each node there are 12 nodal parameters:

$$u_0,\ \varepsilon_{xz}^{(1)},\ \varepsilon_{xz}^{(2)},\ \varepsilon_{xz}^{(3)},\ w_0,\ \frac{dw_0}{dx},\ \varepsilon_{zz}^{(1)},\ \frac{d\varepsilon_{zz}^{(1)}}{dx},\ \varepsilon_{zz}^{(2)},\ \frac{d\varepsilon_{zz}^{(2)}}{dx},\ \varepsilon_{zz}^{(3)},\ \frac{d\varepsilon_{zz}^{(3)}}{dx}.$$

From the extended Hamilton's principle {equation (27) in Part 1 [3]}, written in terms of nodal parameters d_i $(i = 1, 2, ..., 24)$, the following equation of motion of a finite element in terms of the nodal parameters can be derived:

$$\underset{(24\times24)}{[m]}\ \underset{(24\times1)}{\{\ddot{d}\}} + \underset{(24\times24)}{[c]}\ \underset{(24\times1)}{\{\dot{d}\}} + \underset{(24\times24)}{[k]}\ \underset{(24\times1)}{\{d\}} + \underset{(24\times1)}{\frac{\partial U_{nl}}{\partial\{d\}}} = \underset{(24\times1)}{\{r\}}. \tag{52}$$

In this equation, a part U_{nl} of the strain energy is due to the nonlinear terms in the strain-displacement relations (geometric non-linearity of the von Karman type). The expression for U_{nl} is not a quadratic form of the nodal variables, therefore the vector $\frac{\partial U_{nl}}{\partial\{d\}}$ is not linear with respect to the nodal variables. The matrices, which enter into equation (52), were derived with the use of exact integration, performed with a program for symbolic computation, MAPLE. In the finite element analysis, presented in this work, the global damping matrix is not assembled from the element damping matrices. Instead, the proportional damping model is used, in which the global damping matrix $[C]$ is presented as a linear combination of the global stiffness and mass matrices (therefore, the virtual work of the damping forces, as presented by equations (35)–(37) in Part 1 [1], is not used in this finite element formulation, but has only a theoretical importance in formulating the two-dimensional plate-type theory):

$$[C] = \alpha_1[K] + \alpha_2[M], \tag{53}$$

where α_1 and α_2 are constants to be determined from two given logarithmic decrements of damping, δ_1 and δ_2, which correspond to two unequal frequencies of

$$\alpha_1 = \frac{\delta_1\omega_1 - \delta_2\omega_2}{\pi(\omega_1^2 - \omega_2^2)}, \tag{54}$$

vibrations ω_1 and ω_2 by the formulas

$$\alpha_2 = \frac{\omega_1\omega_2(\delta_2\omega_1 - \delta_1\omega_2)}{\pi(\omega_1^2 - \omega_2^2)}. \tag{55}$$

The assembled equations of motion of the whole structure were solved by direct integration with the use of the Newmark method ([4, 5]).

In the post-processing stage of the finite element analysis, the in-plane stresses $\sigma_{xx}^{(k)}$, $\sigma_{xy}^{(k)}$, and $\sigma_{yy}^{(k)}$ are computed with the use of the constitutive equations, which in case of pure plane strain (cylindrical bending), take the form

$$\sigma_{xx}^{(k)} = \overline{C}_{11}^{(k)}\varepsilon_{xx}^{(k)} + \overline{C}_{13}^{(k)}\varepsilon_{zz}^{(k)}, \tag{56}$$

$$\sigma_{xy}^{(k)} = \overline{C}_{16}^{(k)}\varepsilon_{xx}^{(k)} + \overline{C}_{36}^{(k)}\varepsilon_{zz}^{(k)}, \tag{57}$$

$$\sigma_{yy}^{(k)} = \overline{C}_{12}^{(k)}\varepsilon_{xx}^{(k)} + \overline{C}_{23}^{(k)}\varepsilon_{zz}^{(k)}, \tag{58}$$

whereas the transverse stresses $\sigma_{xx}^{(k)}$, $\sigma_{xy}^{(k)}$, and $\sigma_{yy}^{(k)}$ need to be computed by integration of the pointwise equations of motion, which in case of pure plane strain and under the assumption that the plate is perpendicular to the direction of gravity force, take the form

$$\sigma_{xx,x}^{(k)} + \sigma_{xz,z}^{(k)} = \rho^{(k)}\ddot{u}^{(k)}, \tag{59}$$

$$\sigma_{yx,x}^{(k)} + \sigma_{yz,z}^{(k)} = 0, \tag{60}$$

$$\sigma_{zx,x}^{(k)} + \sigma_{zz,z}^{(k)} + \frac{\partial}{\partial x}(\sigma_{xx}^{(k)} w_{,x}^{(k)}) - \rho^{(k)} q = \rho^{(k)}\ddot{w}^{(k)} \qquad (k = 1, 2, 3). \tag{61}$$

If one integrates equations (59)–(61) and satisfies stress boundary conditions on the lower surfaces [equations (8)] and conditions of continuity of the transverse stresses {equations (10) and (11) in Part 1 [1]}, one gets:

$$\sigma_{xz}^{(1)} = \int_{z_1}^{z} (\rho^{(1)}\ddot{u}^{(1)} - {}^{H}\sigma_{xx,x}^{(1)})dz \qquad (z_1 \le z \le z_2), \tag{62}$$

$$\sigma_{xz}^{(2)} = \int_{z_1}^{z_2} (\rho^{(1)}\ddot{u}^{(1)} - {}^{H}\sigma_{xx,x}^{(1)})dz +$$

$$+ \int_{z_2}^{z} (\rho^{(2)}\ddot{u}^{(2)} - {}^{H}\sigma_{xx,x}^{(2)})dz \qquad (z_2 \le z \le z_3), \tag{63}$$

$$\sigma_{xz}^{(3)} = \int_{z_1}^{z_2} (\rho^{(1)} \ddot{u}^{(1)} - {}^{H}\sigma_{xx,x}^{(1)}) dz + \int_{z_2}^{z_3} (\rho^{(2)} \ddot{u}^{(2)} - {}^{H}\sigma_{xx,x}^{(2)}) dz +$$

$$+ \int_{z_3}^{z} (\rho^{(3)} \ddot{u}^{(3)} - {}^{H}\sigma_{xx,x}^{(3)}) dz \qquad (z_3 \le z \le z_4), \tag{64}$$

$$\sigma_{yz}^{(1)}(x,z,t) = -\int_{z_1}^{z} {}^{H}\sigma_{yx,x}^{(1)} dz, \tag{65}$$

$$\sigma_{yz}^{(2)}(x,z,t) = -\int_{z_1}^{z_2} {}^{H}\sigma_{yx,x}^{(1)} dz - \int_{z_2}^{z} {}^{H}\sigma_{yx,x}^{(2)} dz, \tag{66}$$

$$\sigma_{yz}^{(3)}(x,z,t) = -\int_{z_1}^{z_2} {}^{H}\sigma_{yx,x}^{(1)} dz - \int_{z_2}^{z_3} {}^{H}\sigma_{yx,x}^{(3)} dz - \int_{z_3}^{z} {}^{H}\sigma_{yx,x}^{(3)} dz, \tag{67}$$

$$\sigma_{zz}^{(1)} = -\frac{q_l}{b} + \int_{z_1}^{z} \left[\rho^{(1)} (\ddot{w}^{(1)} + g) - \frac{\partial}{\partial x} ({}^{H}\sigma_{xx}^{(1)} w_{,x}^{(1)}) - \sigma_{zx,x}^{(1)} \right] dz, \tag{68}$$

$$\sigma_{zz}^{(2)} = -\frac{q_l}{b} + \int_{z_1}^{z_2} \left[\rho^{(1)} (\ddot{w}^{(1)} + g) - \frac{\partial}{\partial x} ({}^{H}\sigma_{xx}^{(1)} w_{,x}^{(1)}) - \sigma_{zx,x}^{(1)} \right] dz +$$

$$+ \int_{z_2}^{z} \left[\rho^{(2)} (\ddot{w}^{(2)} + g) - \frac{\partial}{\partial x} ({}^{H}\sigma_{xx}^{(2)} w_{,x}^{(2)}) - \sigma_{zx,x}^{(2)} \right] dz, \tag{69}$$

$$\sigma_{zz}^{(3)} = -\frac{q_l}{b} + \int_{z_1}^{z_2} \left[\rho^{(1)} (\ddot{w}^{(1)} + g) - \frac{\partial}{\partial x} ({}^{H}\sigma_{xx}^{(1)} w_{,x}^{(1)}) - \sigma_{zx,x}^{(1)} \right] dz +$$

$$+ \int_{z_2}^{z_3} \left[\rho^{(2)} (\ddot{w}^{(2)} + g) - \frac{\partial}{\partial x} ({}^{H}\sigma_{xx}^{(2)} w_{,x}^{(2)}) - \sigma_{zx,x}^{(2)} \right] dz +$$

$$+ \int_{z_3}^{z} \left[\rho^{(3)} (\ddot{w}^{(3)} + g) - \frac{\partial}{\partial x} ({}^{H}\sigma_{xx}^{(3)} w_{,x}^{(3)}) - \sigma_{zx,x}^{(3)} \right] dz. \tag{70}$$

In the equations (62)–(70), the in-plane stresses with the left superscripts H (which stands for Hook's law) are computed with the use of the Hook's law, i.e.,

from equations (56)–(58). As can be seen from equations (62)–(70), the inertia and nonlinear terms are taken into account in the expressions for the transverse stresses.

With the use of equations (56)–(58) and (62)–(70), all stress components can be expressed in terms of the unknown functions u_0, w_0, $\varepsilon_{xz}^{(1)}$, $\varepsilon_{zz}^{(1)}$, $\varepsilon_{xz}^{(2)}$, $\varepsilon_{zz}^{(2)}$, $\varepsilon_{xz}^{(3)}$, and $\varepsilon_{zz}^{(3)}$. The expressions for the stresses in terms of the unknown functions are not shown explicitly because of their large size. Examples of such expressions are shown in [4].

The values of u_0, w_0, $\dfrac{\partial w_0}{\partial x}$, $\varepsilon_{zz}^{(k)}$, $\dfrac{\partial \varepsilon_{zz}^{(k)}}{\partial x}$, and $\varepsilon_{xz}^{(k)}$ are most accurate at the nodes of the finite element mesh (because these variables are carried as nodal variables), and, for computation of stresses, they can be taken directly from the finite element solution. The second derivatives $\dfrac{\partial^2 w_0}{\partial x^2}$ and $\dfrac{\partial^2 \varepsilon_{zz}^{(k)}}{\partial x^2}$, computed from interpolation polynomials, used in the finite element formulation, are most accurate at the Gauss points. (The locations of the minimal-error points of the derivatives of the field variables within a finite element were calculated with the use of a method presented by Akin [6]). The third derivatives $\dfrac{\partial^3 w_0}{\partial x^3}$ and $\dfrac{\partial^3 \varepsilon_{zz}^{(k)}}{\partial x^3}$, computed from the interpolation polynomials, are constant over the element's length and are most accurate in the middle of the finite element. The derivatives $\dfrac{\partial^4 w_0}{\partial x^4}$, $\dfrac{\partial^4 \varepsilon_{zz}^{(2)}}{\partial x^4}$, $\dfrac{\partial^2 u_0}{\partial x^2}$, and $\dfrac{\partial^2 \varepsilon_{xz}^{(k)}}{\partial x^2}$, taken as derivatives of the interpolation polynomials, which are used in the finite element formulation, are equal to zero that can be wrong for a particular problem. Therefore, these derivatives are computed numerically at the nodal points by a finite difference scheme, using the nodal values of w_0, $\varepsilon_{zz}^{(k)}$, u_0, and $\varepsilon_{xz}^{(k)}$, obtained from the finite element solution. So, there are no points within the finite element where all the derivatives of the field variables are most accurate simultaneously. Therefore, in order to compute stresses, the average (over the element's length) values of the field variables and their derivatives are evaluated, as average values at the points where these quantities are most accurate, and then substituted into the expressions for the stresses, producing average (over the element's length) values of stresses.

The computation of the transverse stresses from the equations of motion allows one to satisfy the stress boundary conditions on the upper and lower surfaces of the plate, and the conditions of continuity of the transverse stresses at the interfaces between the faces and the core of the sandwich plate and between the plies with different material properties within the faces [2]. The computation of the transverse stresses by integration of the pointwise equilibrium equations is demonstrated, for example, in [4] and some other works included in the bibliography of therein. The fact that the computation of the transverse stresses by integration of the pointwise equilibrium equations (or equations of motion) allows for the satisfaction of the stress boundary conditions not only on one of the external surfaces (upper or lower), but on both of them, was explained in [2].

In most common cases of boundary conditions, i.e., simply supported, clamped, and free edges of the plate, the nodal values of the transverse strains $\varepsilon_{xz}^{(1)}$, $\varepsilon_{zz}^{(1)}$, $\varepsilon_{xz}^{(2)}$, $\varepsilon_{zz}^{(2)}$, $\varepsilon_{xz}^{(3)}$, and $\varepsilon_{zz}^{(3)}$ and their derivatives need not be specified at the edges.

Time Integration with Account of Damage Progression. When a failure occurs in a single layer of a composite laminate, a composite structure can still carry a load. Therefore, a subsequent failure prediction is required to determine a dynamic response of the structure in the presence of some damage. This problem is dealt with by assuming that within a finite element where the damage occurs, the original material characteristics of the damaged ply can be replaced with degraded material characteristics. The degraded material properties are assumed to be small fractions of the properties of the undamaged material, but not equal to zero, in order to avoid ill-conditioning of the finite element equations. For example, a degraded value of the Young's modulus E_d of the damaged ply within a finite element is computed as

$$E_{1d} = (src)E_1, \tag{71}$$

where E_1 is an original value of the Young's modulus and (src) is a stiffness reduction coefficient.

The face sheets of the sandwich plate are made of laminated composite plates, that can fail in different modes: due to matrix cracking, fiber fracture, fiber matrix debonds and delamination. Therefore, for accurate prediction of failure in the face sheets, one needs to use a failure criterion that takes account of the microstructure of the composite laminates and the variety of modes of failure that can occur due to this microstructure. A set of failure criteria, designed for this purpose, were suggested by Hashin [7]. Therefore, for the face sheets, Hashin's criteria are used in this study.

The core of the sandwich plate, made of polymeric foam or a honeycomb structure, is modelled as a homogeneous isotropic or transversely isotropic medium. Such a medium has fewer modes of failure, namely crushing under compression and cracking under tension. Therefore, for the failure analysis of the core, it is more appropriate to use a failure criterion that does not take account of the microstructure of the material. One such criterion is the Tsai–Wu criterion [8, 9] and it is used for the core in this study. The core, that is uniform before the beginning of the damage, becomes nonuniform in the thickness direction (as well as in longitudinal direction) when the damage starts to progress in the thickness direction. For this reason, the core is divided into the nominal layers, and a check of the failure criterion in the middle of thickness of each such layer is carried out.

In case of crushing of the core of the sandwich plate and tension modes of failure, the stiffness reduction coefficients (src) for all material constants are set to be as small as possible, but their smallness is limited by the need to avoid numerical difficulties that can be caused by the large difference of values of material constants of adjacent finite elements. Such values of the stiffness reduction coefficients are found by numerical experimentation. In the numerical examples presented hereafter, the stiffness reduction coefficient (src) is set equal to 0.001 in case of crushing of the core of the sandwich plate and failure in

tension, and 0.01 in case of fiber failure in compression in the face sheets. The stiffness reduction coefficient, associated with the fiber failure in compression, is set equal to a larger value, because the compressive fiber mode of failure is interpreted as buckling of fibers in the matrix [10]. It is assumed that if the buckling of the fibers occurs, the layer still has some residual strength.

At each time step, the average (over a finite element length) stresses in each layer within each element are used in the failure criteria.

Now, the *algorithm of taking account of damage progression* will be presented without details of how it is imbedded into the time integration scheme (the details will be presented subsequently).

1) At each time step of time integration, compute average (over an element length) stresses σ_{xx}, σ_{xy}, σ_{yy}, σ_{xz}, σ_{yz}, and σ_{zz} in the problem coordinate system in all finite elements, in the middle of each ply of the face sheets (at $z = (\xi_k + \xi_{k+1})/2$) and in the middle of each nominal layer of the core (computation of average stresses is discussed above).

2) Transform the stresses to the principle material coordinates, i.e., compute σ_{11}, σ_{22}, σ_{33}, σ_{12}, σ_{13}, and σ_{23}.

3) Substitute the stresses in the material coordinate system into the failure criteria. The Hashin criteria [7] are used for the face sheets and the Tsai–Wu criterion [8, 9] is used for the core. If the failure occurs, reduce the appropriate engineering constants of the face sheets and the core using the methods described earlier.

4) By the use of the modified values of engineering elastic constants, for each layer of each finite element that fails, recompute elastic constants ${}^{\alpha}\overline{C}_{ij}^{(k)}$, element stiffness matrices, the global stiffness matrix, and restart the analysis at the same time step, i.e., return to the step 1.

Such a method is used because when failure occurs, the stress field changes instantly due to the change of material properties. This redistribution of the stresses may cause additional failure to occur. Therefore, in case of failure, the time incrementation must be stopped, and analysis must be run again for the same time interval to determine the new failure. If the new failure does not occur, the analysis can go on to the next time step.

5) If failure does not occur, proceed to the next time step. Analysis goes on for a number of time steps, specified by a user.

Now, the details will be presented on how the damage progression algorithm is imbedded into the time integration scheme of the system equations of motion

$$[M]\{\ddot{\Theta}\} + [C]\{\dot{\Theta}\} + [K]\{\Theta\} + \{Q\} = \{P\}, \tag{72}$$

with the use of the Newmark method [5]. In equation (72), the matrix $[K]$ is the system stiffness matrix, whose components do not depend on the nodal unknowns Θ_i, and $\{Q\}$ is a nonlinear part of the internal force vector, whose components are defined as $\dfrac{\partial (U_{nl})_{system}}{\partial \Theta_i}$, where $(U_{nl})_{system}$ is the whole system's part of the strain energy that is not quadratic with respect to the nodal unknowns. The part of the strain energy $(U_{nl})_{system}$ appears due to the nonlinear terms in the von

Karman strain-displacement relations [11]. Thus, the problem being solved numerically is geometrically nonlinear.

Let us introduce the following notations:

$\{\Theta\}\big|_{t=t_n} \equiv \{\Theta\}_n$ – vector of nodal variables, evaluated at moment of time t_n,

$\{\Theta\}\big|_{t=t_{n+1}} \equiv \{\Theta\}_{n+1}$ – vector of nodal variables, evaluated at moment of time t_{n+1},

$\tau \equiv t_{n+1} - t_n$.

With the use of the Taylor series expansion, vectors $\{\Theta\}_{n+1}$ and $\{\dot{\Theta}\}_{n+1}$ can be written in the form

$$\{\Theta\}_{n+1} \approx \{\Theta\}_n + \tau\{\ddot{\Theta}\}_n + \tau^2\left(\frac{1}{2} - \beta\right)\{\ddot{\Theta}\}_n + \tau^2\beta\{\ddot{\Theta}\}_{n+1}, \tag{73}$$

$$\{\ddot{\Theta}\}_{n+1} \approx \{\ddot{\Theta}\}_n + \tau(1-\gamma\tau)\{\ddot{\Theta}\}_n + \tau^2\gamma\{\ddot{\Theta}\}_{n+1}, \tag{74}$$

where β and γ are free parameters that control the accuracy and stability of the method. In the example problems considered below, the values of these parameters were chosen to be $\beta = 1/4$ and $\gamma = 1/2$, which correspond to the method of constant mean acceleration. Such a method is unconditionally stable and provides a satisfactory accuracy.

Equations of motion (72), evaluated at a moment of time t_{n+1}, are

$$[M]\{\ddot{\Theta}\}_{n+1} + [C]\{\ddot{\Theta}\}_{n+1} + [K]\{\Theta\}_{n+1} + \{Q\}_{n+1} = \{P\}. \tag{75}$$

In equations (72) and (75), the load vector $\{P\}$ is due to the gravity force, so it does not depend on time and, therefore, does not have the subscript n. Substitution of equations (73) and (74) into equation (75) and simple transformations yield:

$$[\hat{K}]\{\Theta\}_{n+1} + \{Q\}_{n+1} = \{\hat{F}\}_n, \tag{76}$$

where

$$[\hat{K}] \equiv [K] + \frac{1}{\tau^2\beta}[M] + \frac{\gamma}{\beta}[C], \tag{77}$$

$$\{\hat{F}\}_n = \{P\} - [C](\{\ddot{\Theta}\}_n + \tau(1-\gamma\tau)\{\ddot{\Theta}\}_n) +$$

$$+\left(\frac{1}{\tau^2\beta}[M] + \frac{\gamma}{\beta}[C]\right)\left(\{\Theta\}_n + \tau\{\dot{\Theta}\}_n + \tau^2\left(\frac{1}{2} - \beta\right)\{\ddot{\Theta}\}_n\right). \tag{78}$$

Now, assuming that the values of $\{\Theta\}_n$, $\{\ddot{\Theta}\}_n$, and $\{\ddot{\Theta}\}_n$ are known, one needs to find the values of $\{\Theta\}_{n+1}$, $\{\ddot{\Theta}\}_{n+1}$, and $\{\ddot{\Theta}\}_{n+1}$. Components of vector $\{Q\}_{n+1}$, that enters into equation (76), depend nonlinearly on components of the vector of nodal parameters $\{\Theta\}_{n+1}$. Therefore, equation (76) is a nonlinear

system of algebraic equations with respect to components of the vector $\{\Theta\}_{n+1}$. These nonlinear equations are solved by a direct iteration (Picard) method [4].

The direct iteration method is based on computing a sequence of vectors

$$\{\Theta\}_{n+1}^{(1)},\ \{\Theta\}_{n+1}^{(2)},\ \{\Theta\}_{n+1}^{(3)},\ \ldots \tag{79}$$

by solving a system of linear algebraic equations

$$[\hat{K}]\{\Theta\}_{n+1}^{(r+1)} = \{\hat{F}\}_n - \{Q\}_{n+1}^{(r)}, \tag{80}$$

where the vector $\{Q\}_{n+1}^{(r)}$ is the vector $\{Q\}_{n+1}$ evaluated at $\{\Theta\}_{n+1} = \{\Theta\}_{n+1}^{(r)}$, i.e., evaluated with the use of values of nodal parameters Θ_i obtained at the rth iteration. The components of the matrix $[\hat{K}]$ and the vector $\{\hat{F}\}_n$ do not depend on the unknowns, i.e., on the components of the vector $\{\Theta\}_{n+1}$. If the sequence of vectors $\{\Theta\}_{n+1}^{(1)},\ \{\Theta\}_{n+1}^{(2)},\ \{\Theta\}_{n+1}^{(3)}, \ldots$ converges to some vector $\{\tilde{\Theta}\}_{n+1}$, then this vector $\{\tilde{\Theta}\}_{n+1}$ is a solution of the system of algebraic equations (76). In this numerical implementation

$$\{\Theta\}_{n+1}^{(1)} = \{0\}, \tag{81}$$

the first term of the iteration sequence $\{\Theta\}_{n+1}^{(1)},\ \{\Theta\}_{n+1}^{(2)},\ \{\Theta\}_{n+1}^{(3)}, \ldots$ is set equal to a zero-vector at all time intervals for $n = 1, 2, 3, \ldots$. Iteration is stopped if a norm of vector $\{\Theta\}_{n+1}^{(r+1)} - \{\Theta\}_{n+1}^{(r)}$ (a difference of solution vectors in two successive approximations), divided by the norm of vector $\{\Theta\}_{n+1}^{(r+1)}$ is less than some number (tolerance):

$$\frac{\left\| \{\Theta\}_{n+1}^{(r+1)} - \{\Theta\}_{n+1}^{(r)} \right\|}{\left\| \{\Theta\}_{n+1}^{(r+1)} \right\|} < tolerance. \tag{82}$$

As a norm of a vector, a square root of the sum of the squares of its components was used. Let $(\Theta_i)_{n+1}^{(r)}$ be an ith component of the approximate solution vector obtained in an iteration with a number r at a moment of time with a number $n+1$. Then the criterion (82) for stopping the iterations will be written as follows:

$$\frac{\sqrt{\sum_i [(\Theta_i)_{n+1}^{(r+1)} - (\Theta_i)_{n+1}^{(r)}]^2}}{\sqrt{\sum_i [(\Theta_i)_{n+1}^{(r+1)}]^2}} < tolerance. \tag{83}$$

In the example problems considered below, it is set: $tolerance = 1 \cdot 10^{-4}$.

Thus, *in the problems with the damage progression taken into account*, the algorithm of the Newmark [5] time integration scheme, combined with the direct

iteration method of solving the nonlinear algebraic equations (76), can be summarized as follows:

I) At the first time interval $[t_1, t_2]$, set the vectors of initial generalized displacements $\{\Theta\}_1$ and velocities $\{\dot{\Theta}\}_1$ equal to the values specified in initial conditions. The vector $\{\ddot{\Theta}\}_1$ of initial generalized accelerations is found from the equation (75), where n is set equal to zero:

$$[M]\{\ddot{\Theta}\}_1 + [C]\{\dot{\Theta}\}_1 + [K]\{\Theta\}_1 + \{Q\}_1 = \{P\}. \tag{84}$$

This is a system of linear algebraic equations with respect to components of the vector $\{\ddot{\Theta}\}_1$.

II) At the nth time interval $[t_n, t_{n+1}]$, the vectors $\{\Theta\}_n$, $\{\dot{\Theta}\}_n$, $\{\ddot{\Theta}\}_n$, and $\{Q\}_n$ are known, and it is necessary to find the vectors $\{\Theta\}_{n+1}$, $\{\dot{\Theta}\}_{n+1}$, $\{\ddot{\Theta}\}_{n+1}$, and $\{Q\}_{n+1}$. For this purpose, the following algorithm is used.

1) Set the iteration counter r equal to 1, and set the initial approximation for the vector $\{\Theta\}_{n+1}$ to be a zero-vector:

$$\{\Theta\}_{n+1}^{(1)} = \{0\}. \tag{85}$$

2) Evaluate $\{Q\}_{n+1}^{(r)}$, i.e., evaluate $\{Q\}_{n+1}$ at $\{\Theta\}_{n+1} = \{\Theta\}_{n+1}^{(r)}$ and solve a linear system of algebraic equations for the components of the vector $\{\Theta\}_{n+1}^{(r+1)}$

$$[\hat{K}]\{\Theta\}_{n+1}^{(r+1)} = \{\hat{F}\}_n - \{Q\}_{n+1}^{(r)}. \tag{86}$$

Evaluate the acceleration vector of the current iteration (iteration with number $r+1$) by the formula

$$\{\ddot{\Theta}\}_{n+1}^{(r+1)} = \frac{1}{\tau^2\beta}\left(\{\Theta\}_{n+1}^{(r+1)} - \{\Theta\}_n - \tau\{\dot{\Theta}\}_n - \tau^2\left(\frac{1}{2} - \beta\right)\{\ddot{\Theta}\}_n\right) \tag{87}$$

[equation (87) is obtained by expressing $\{\ddot{\Theta}\}_{n+1}$ from equation (73)]. Evaluate the velocity vector of the current iteration (iteration with number $r+1$) by the formula

$$\{\dot{\Theta}\}_{n+1}^{(r+1)} = \{\dot{\Theta}\}_n + \tau(1-\gamma\tau)\{\ddot{\Theta}\}_n + \tau^2\gamma\{\ddot{\Theta}\}_{n+1}^{(r+1)} \tag{88}$$

[equation (88) is obtained from equation (74)].

3) Check if the vectors $\{\Theta\}_{n+1}^{(r+1)}$ and $\{\Theta\}_{n+1}^{(r)}$ satisfy the convergence criterion of equation (83).

If the convergence criterion is not satisfied, then begin a new iteration within this time interval, i.e., set $r = r+1$ and go back to the step 2. If the convergence criterion is satisfied, go to the next step.

4) Set the vector of nodal parameters and the vectors of the first and second time derivatives of the nodal parameters equal to the corresponding vectors

obtained in the iteration at which the convergence criterion of the step 3 was satisfied, i.e., set

$$\{\Theta\}_{n+1} = \{\Theta\}_{n+1}^{(r+1)}, \tag{89}$$

$$\{\dot{\Theta}\}_{n+1} = \{\dot{\Theta}\}_{n+1}^{(r+1)}, \tag{90}$$

$$\{\ddot{\Theta}\}_{n+1} = \{\ddot{\Theta}\}_{n+1}^{(r+1)} \tag{91}$$

for use in the next time step and for computation of stresses at $t = t_{n+1}$.

5) Compute average stresses in all plies of each finite element at $t = t_{n+1}$, using the vectors $\{\Theta\}_{n+1}$, $\{\ddot{\Theta}\}_{n+1}$, and $\{\ddot{\Theta}\}_{n+1}$, obtained in the 4th step. Substitute these stresses into the failure criteria. In a ply of a finite element, modify material elastic constants of this ply, modify the element stiffness matrix $[k]$ and the nonlinear internal force vector $\{q\}_{n+1} = \left(\frac{\partial U_{nl}}{\partial\{\Theta\}}\right)_{n+1}$ of the finite element to which the damaged ply belongs and assemble the global stiffness matrix $[K]$ and global nonlinear internal force vector $\{Q\}_{n+1}$ with account of modifications to the element stiffness matrices and element nonlinear internal force vectors due to the damage. Then go to the step 2, i.e., recompute vectors $\{\Theta\}_{n+1}$, $\{\dot{\Theta}\}_{n+1}$, and $\{\ddot{\Theta}\}_{n+1}$ and stresses at the same moment of time.

When failure occurs, the stress field changes instantly due to the change of material properties. This redistribution of the stresses may cause additional failure to occur. Therefore, in case of failure, the time incrementation must be stopped and analysis must be run again for the same time interval to determine the new failure. If the new failure does not occur, the analysis can go on to the next time step.

If failure does not occur, set $n = n + 1$, i.e., go to the next time interval.

Analysis goes on for a number of time steps, specified by a user.

Example Problems. In some problems, when the plates are loaded on both the upper and lower surfaces, or when the plates are on elastic foundations, transverse compressibility of the sandwich plates can not be neglected. In the proposed finite element formulation, the transverse compressibility is taken into account by assuming that the direct transverse strain ε_{zz} is not equal to zero, and by including this strain into the expression for the strain energy. In the following example, a sandwich plate is considered, with a rigid body on its upper surface, under its impact against an elastic Winkler foundation, and demonstrate that the change of the plate's height during this impact can be captured by the finite element model. In the finite element formulation, the presence of the rigid body on the upper surface is taken account by including a kinetic energy of the rigid body into the Hamilton's principle. Example problems, considered below, are solved with the use of the geometrically nonlinear formulation. Forty finite elements are used in all example problems.

So far, the numerical implementation of the theory is performed for the case of cylindrical bending only, which occurs if the width of the plate is larger than the length, and the load on the surface is uniformly distributed along the width. In

this case, the stress distribution and stiffness degradation are uniform in the width direction.

Let us consider an example of a sandwich plate with laminated composite face sheets, made of AS4/3501-6 material, and a honeycomb core, made of Nomex HRH10-1/8-4.0. The material properties of the face sheets and the core, used in the example problems, are listed below. Elastic constants of the face sheets: $E_1 = 144.8 \cdot 10^9$ N/m^2, $E_2 = 9.7 \cdot 10^9$ N/m^2, $E_3 = 9.7 \cdot 10^9$ N/m^2, $G_{23} = 3.6 \cdot 10^9$ N/m^2, $G_{13} = 6.0 \cdot 10^9$ N/m^2, $G_{12} = 6.0 \cdot 10^9$ N/m^2, $\nu_{23} = 0.34$, $\nu_{13} = 0.3$, and $\nu_{12} = 0.3$. Material strengths of the face sheets: $X_T = 2.17 \cdot 10^9$ N/m^2, $X_C = 1.72 \cdot 10^9$ N/m^2, $Y_T = 53.8 \cdot 10^6$ N/m^2, $Y_C = 205.5 \cdot 10^6$ N/m^2, $Z_T = 53.8 \cdot 10^6$ N/m^2, $Z_C = 205.5 \cdot 10^6$ N/m^2, $S_{23} = 89.3 \cdot 10^6$ N/m^2, $S_{13} = 120.7 \cdot 10^6$ N/m^2, and $S_{12} = 120.7 \cdot 10^6$ N/m^2, where X_T, X_C, Y_T, Y_C, Z_T, and Z_C are the material strengths in tension and compression along 1, 2, 3 directions, and S_{23}, S_{13}, and S_{12} are the shear strengths in the 23, 13 and 12 planes. Elastic constants of the core: $E_1 = 80.4 \cdot 10^6$ N/m^2, $E_2 = 80.4 \cdot 10^6$ N/m^2, $E_3 = 1005 \cdot 10^6$ N/m^2, $G_{23} = 75.8 \cdot 10^9$ N/m^2, $G_{13} = 120.6 \cdot 10^6$ N/m^2, $G_{12} = 32.2 \cdot 10^6$ N/m^2, $\nu_{23} = 0.02$, $\nu_{13} = 0.02$, and $\nu_{12} = 0.25$. Material strengths of the core: $Z_C = 3.83 \cdot 10^6$ N/m^2, $S_{23} = 142.3 \cdot 10^6$ N/m^2, and $S_{13} = 177.9 \cdot 10^6$ N/m^2. Both face sheets have the same thickness 0.0025 m, and each of them consists of 25 plies with 0°/90° lay-up. The thickness of the core is 0.04 m. On the upper surface of the plate there is a rigid body of mass 500 kg, located symmetrically with respect to the middle of the plate's span, and has the length 0.2 m.

The modulus of the elastic Winkler foundation in the example problem, represented by Fig. 1, is $6.7864 \cdot 10^8$ Pa/m (clay). A time increment, used in numerical integration of equations of motion (72), is chosen to be $1 \cdot 10^{-4}$ s. A plate, falling on the elastic foundation with velocity 30 m/s, is considered. The analysis of the response [time integration of the equations of motion (72)] in this and all subsequent example problems begins at the moment of time when the falling plate touches the elastic foundation. Figure 1 shows the transverse displacement of the lower surface of the plate as a function of time, computed with account of damage (solid line) and without account of damage (dashed line). In the analysis with the account of damage, the amplitude of vibration is higher. This is expected because the stiffness of the damaged structure is lower.

Figure 2 shows the transverse displacement of the plate falling on the foundation with the smaller modulus, $6.7864 \cdot 10^7$ Pa/m. All other conditions are the same as in the previous example. It can be seen that in case of the lower modulus of the foundation, the amplitude of the transverse displacement is higher. So, the effect of the foundation stiffness is taken into account properly.

Figure 3a and 3b show results of stress analysis with and without account of damage progression of the same sandwich plate under the impact against the elastic foundation. All conditions of the problem are the same as in the previous example. As seen in Fig. 3a, when the fiber breakage occurs, the in-plane direct

stress σ_{xx} reduces drastically, due to the degradation of the material characteristics, associated with the in-plane direction. At the moment of time $t = 0.016$ s, when stress σ_{zz} at the lower surface of the damaged plate (i.e., force of interaction between the plate and the elastic foundation per unit area) reaches a zero value (Fig. 3b), the plate loses contact with the elastic foundation and bounces up into the air. Therefore, this and all other graphs are to be considered only for the time interval during which the stress σ_{zz} at the lower surface of the plate is not positive (time interval $0 \le t \le 0.016$ s for the Fig. 3b), unless the plate is glued to the elastic foundation at the moment of initial contact (i.e. forced to stay in contact with the foundation). If the plate is forced to stay in contact with the foundation, all the graphs are correct for any time duration.

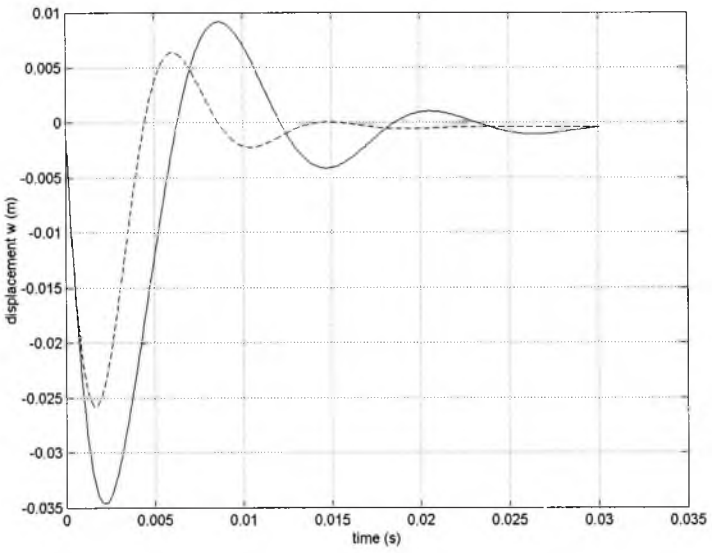

Fig. 1. Transverse displacement w (at $x = L/2$, $z = -h/2$) as a function of time in a sandwich plate dropped on elastic foundation with initial velocity 30 m/s. The foundation modulus is $6.7864 \cdot 10^8$ Pa/m (clay). Here and in Figs. 2, 3: dashed line represents results of analysis without account of damage, solid line – with damage included.

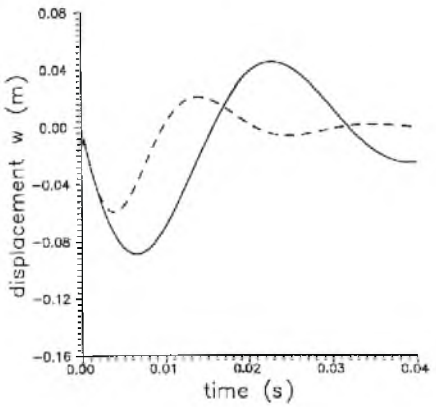

Fig. 2. Transverse displacement w (at $x = L/2$, $z = -h/2$) as a function of time in a sandwich plate dropped on elastic foundation with velocity 30 m/s. The foundation modulus is $6.7864 \cdot 10^7$ Pa/m (sand).

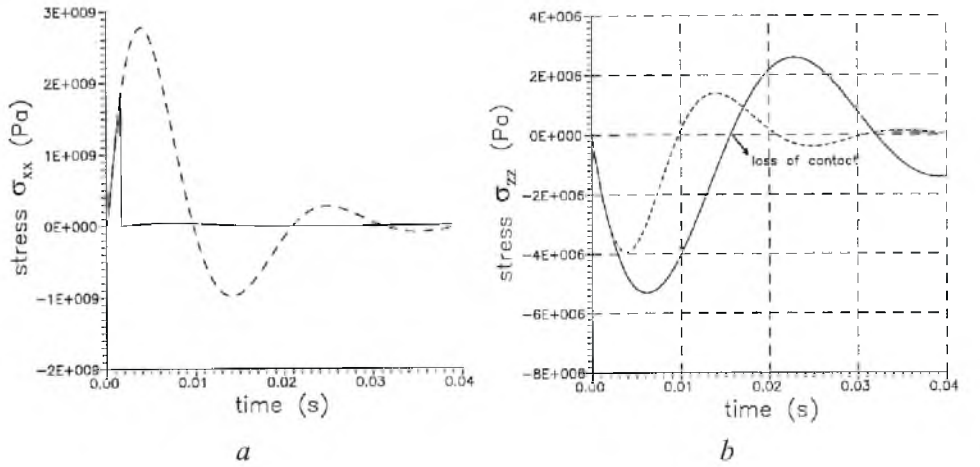

Fig. 3. Stresses σ_{xx} (a) and σ_{zz} (b) at $x = L/2$, $z = -h/2$ as a function of time in a sandwich plate dropped on elastic foundation with initial velocity 30 m/s. The foundation modulus is $6.7864 \cdot 10^7$ Pa/m (sand).

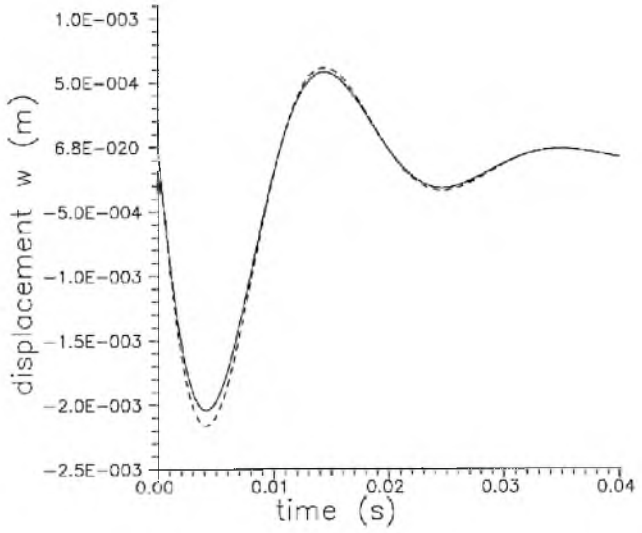

Fig. 4. Transverse displacement (at $x = -L/2$) as a function of time in a sandwich plate with a mass on its upper surface, dropped on elastic foundation with initial velocity 1 m/s. The foundation modulus is $6.7864 \cdot 10^7$ Pa/m (sand). The solid line represents displacement of the lower surface, the dashed line – displacement of the upper surface. Under this initial velocity damage does not occur.

Figure 4 shows the transverse displacement of the plate falling on the foundation with the smaller initial velocity 1 m/s. All other conditions are the same as in the previous example. Comparison of Figs. 2 and 4 shows that the effect of the initial velocity on the response is captured properly: the lower initial velocity causes the lower amplitude of vibration. Figure 4 shows also that the amplitude of the transverse displacement of the upper surface is higher, and this shows the capability of the model to capture the compressibility of the plate in the transverse direction.

Conclusions. The theory of the sandwich plate, presented in this paper, has a wide range of applicability. It can be used for analysis of sandwich plates with large and small thickness-to-length ratios, with thick and thin face sheets, with transversely rigid and transversely flexible face sheets and cores. The proposed finite element formulation allows one to compute accurately all stress components, both in-plane and transverse, without using finite element models with three-dimensional elements. The geometrical non-linearity of the finite element formulation allows for a nonlinear transient analysis of a sandwich composite plate undergoing moderate rotations. The algorithm of taking account of damage progression in a dynamic problem is incorporated into the computational scheme, based on the geometrically nonlinear formulation.

Резюме

Для випадку товстої багатошарової панелі з поверхневими шарами з композитного ламіната запропоновано розрахункову схему в рамках теорії пластин із використанням спрощених уявлень, що описані у повідомленні 1. Алгоритм розрахунку динамічної задачі, в якому приймається до уваги розвиток пошкоджень у матеріалі, використовується у розрахунковій схемі, що базується на геометрично нелінійному формулюванні задачі, для аналізу умов руйнування багатошарової панелі, що зазнає ударного навантаження при падінні на грунт.

1. V. Y. Perel, "Nonlinear dynamic finite element analysis of thick transversly flexible sandwich panel on elastic foundation with account of damage progression in time. Part 1. Three-dimensional formulation and two-dimensional plate theory," *Probl. Prochn.*, No. 2, 92–106 (2005).
2. S. G. Lekhnitskii, *Theory of Elasticity of an Anisotropic Body*, Holden-Day, San Francisco (1963).
3. V. Y. Perel, *Three-Dimensional Dynamic Stress Analysis of Sandwich Panels*, Ph.D. Dissertation, AFIT/DS/ENY/00-02, Air Force Institute of Technology (2000), https://research.maxwell.af.mil/papers/ay2001/afit/afit-ds-eny-00-02.pdf.
4. J. N. Reddy, *Mechanics of Laminated Composite Plates and Shells: Theory and Analysis*, CRC Press, Boca Raton, Florida (2003).
5. N. M. Newmark, "A method of computation for structural dynamics," *Trans. ASCE*, **127**, 1406–1435 (1959).
6. J. E. Akin, *Finite Element Analysis for Undergraduates*, Academic Press, London (1986).
7. Z.-H. Hashin, "Failure criteria for unidirectional fiber composites," *J. Appl. Mech.*, **47**, 329–334 (1980).
8. V. D. Azzi and S. W. Tsai, "Anisotropic Strength of Composites," *Exp. Mech.*, **5**, 283–288 (1965).
9. E. M. Wu, "Phenomenological anisotropic failure criterion," *Compos. Mater.*, **2**, 353–431 (1974).

10. L. J. Broutman and R. H. Krock, *Modern Composite Materials*, Addison-Wesley Publishing Company, Reading, Massachusetts, (1967).

11. T. von Karman, "Festigkeitsprobleme in Maschinenbau," Encycl. Math. Wissenschaften (1910), IV/4C, SS. 311–385.

Received 09. 11. 2004